2009 American Control Conference
Hyatt Regency Riverfront, St. Louis, MO, USA
June 10-12, 2009

A New Nonlinear-Filter-Based Modulation/Demodulation Technique for Chaotic Communication

Xin Wang and Edwin E. Yaz

Abstract --- **A novel modulation/demodulation technique for digital chaotic communications using nonlinear filtering is proposed. The performance of this technique is compared in simulation with the existing nonlinear filtering based chaotic communication schemes for three different nonlinear estimators. The feasibility of the proposed technique is verified by theoretical analysis and computer simulation. The result is also compared with the theoretical bit error rate performance bound for chaotic communications.**

I. INTRODUCTION

In February 2003, the FCC released 3.1 GHz to 10.6 GHz, a radio bandwidth of 7.5 GHz (commonly known as Ultra-Wideband Communications) for public use. The UWB signal has the bandwidth of about 20% to 25% of the center frequency, which is significantly different from traditional communication techniques. To better utilize this bandwidth resource, the IEEE 802.15 committee has led to the standardization of UWB communications. The IEEE 802.15.4.a standard focuses on low bit rate Wireless Personal Area Network (WPAN) with high precision ranging/location capability, low power consumption and low cost [1]-[3]. Many chaotic modulation techniques have been proposed in recent literature to satisfy the above requirement. However, insufficient synchronization, interference and time varying channel characteristics are among the most significant limitations in those approaches. The most popular schemes include DCSK, CSK and COOK. The Differential Chaos Shift Keying (DCSK) contains a basis function in half of its symbol period which can be used as the reference signal; this exact timing requirement may not be feasible for applications. The Chaotic Shift Keying (CSK) scheme uses coherent reception, which needs precise synchronization at every sampling time step and its basis function cannot be regenerated at the receiver unless the initial condition of the chaotic signal generator used at the transmitter is available. This critical timing requirement makes CSK impractical in use. The Chaotic On-Off Keying (COOK) does not requite precise synchronization. But the performance of this scheme degrades rapidly in the multipath channel. Also, interference can be a serious limitation for COOK, since it uses a bit-energy based demodulator and interference can be mistaken as the actual message.

Xin Wang and Edwin E. Yaz are with the Department of Electrical and Computer Engineering, Marquette University, Milwaukee, WI 53201, USA. Email: {xin.wang, edwin.yaz}@marquette.edu

Since chaotic signals are generated by nonlinear systems and can be thought of as state variables of such systems, nonlinear filtering techniques for state estimation based on noisy measurements provide us with important tools for the demodulation in chaotic communication systems. Currently available nonlinear filtering based chaotic communication techniques use Extended Kalman Filter (EKF) in two schemes: chaotic communications based on state/parameter estimation technique [4][5] and chaotic communications using two maps technique [6]. The former technique uses two tent maps with different parameters, and by estimating the parameter to decide which symbol is transmitted. And the latter uses two chaotic maps for transmission corresponding to different symbols. By estimating which map is used based on a bank of filters and comparing estimation errors, the corresponding binary information transmitted can be estimated. However, these techniques may not provide us satisfactory Bit Error Rate (BER) versus Signal to Noise Ratio (SNR) performance either.

This work aims to propose a novel modulation/ demodulation technique using nonlinear filtering. Then three nonlinear estimation techniques, namely, EKF, State Dependent Riccati Equation (SDRE) estimator [8] and Unscented Kalman Filter (UKF) [9] are introduced for demodulation. Comparative simulation studies involving BER vs. SNR and theoretical analysis are included in this paper. Finally, we compare our new results with the theoretical BER performance bound for chaotic communications.

II. A NOVEL CHAOTIC COMMUNICATION MODULATION/DEMODULATION SCHEME

The discrete time chaotic communication system and measurement model can be represented by:

$$\begin{cases} x_{k+1} = f(x_k, a) \\ y_k = C \cdot x_k + w_k \end{cases} \tag{1}$$

where

$f(x_k, a)$ chaotic map with parameter a

x_k state variable of the chaotic map at the discrete time step k

y_k received Additive White Gaussian Noise (AWGN) corrupted signal

C amplifier gain

w_k AWGN measurement noise with zero mean and W covariance

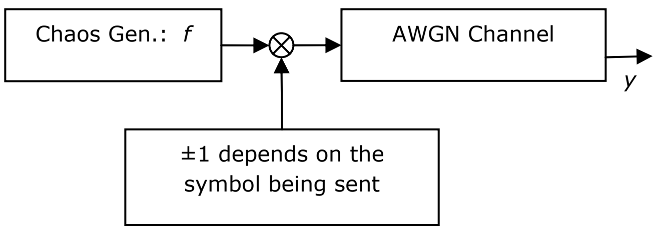

Fig.1. Transmitter design

The modulator part of our new chaotic communication scheme is given in Fig.1. Notice that only one chaotic map generator f is used. During each symbol period, when the information symbol "+1" is sent, we modulate the symbol by the chaotic signal. When symbol "–1" is sent, the inverted version of the chaotic signal is transmitted. Essentially, the transmitter uses the binary symbol ±1 multiplied with the chaotic signal. If "+1" is transmitted, the following model is applicable:

$$\begin{cases} x_{k+1} = f(x_k) \\ y_k = +1 \cdot x_k + w_k \end{cases} \tag{2}$$

In the detector, Filter 1 is designed based on this model.

Similarly, if "-1" is transmitted, the following model applies:

$$\begin{cases} x_{k+1} = f(x_k) \\ y_k = -1 \cdot x_k + w_k \end{cases} \tag{3}$$

In the detector, Filter 2 is designed based on this model.

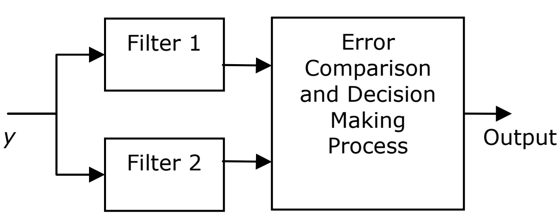

Fig.2. Receiver design

During each symbol period, either the chaotic signal itself or its inverted version is transmitted, i.e., only one of the models, either Eqn. (2) or Eqn. (3) applies. The receiver part of our new scheme is shown in Fig.2. Two nonlinear filters use these different dynamic models are estimating the received signal separately. Only one filter, which has the matched model for the transmitted signal, converges to the correct chaotic signal during each symbol period, while the other filter, which has the unmatched model, produces much more error. In this case, by comparing the estimation errors during each symbol period, we can make a decision about which message is being transmitted. We use three nonlinear filtering approaches: EKF, SDRE and UKF in a comparative study for state estimation.

Detection Using EKF

In the first method, we set up an EKF estimator using the following equations:

Propagation from time step k to (k+1):

In the time update part, the state estimate and the local estimation error covariance is computed by:

$$\begin{cases} \hat{x}_{k+1}^- = f\left(\hat{x}_k^+, \hat{a}_k\right) \\ P_{k+1}^- = A_k \cdot P_k^+ \cdot A_k^T \end{cases} \tag{4}$$

The measurement update of the state and local estimation covariance is as follows:

$$\begin{cases} K_{k+1} = P_{k+1}^- \cdot C^T \cdot (C \cdot P_{k+1}^- \cdot C^T + W)^{-1} \\ \hat{x}_{k+1}^+ = \hat{x}_{k+1}^- + K_{k+1}(y_{k+1} - C \cdot \hat{x}_{k+1}^-) \\ P_{k+1}^+ = (I - K_{k+1} C) P_{k+1}^- \end{cases} \tag{5}$$

where,

$A_k = \left. \partial f / \partial x_k \right|_{\hat{x}_k}$ Jacobian matrix

$\hat{x}_k^-$ a priori estimated chaotic state at time step k with local estimation error covariance P_k^-

$\hat{x}_k^+$ the posteriori estimated chaotic state at time step k with local estimation error covariance P_k^+

C the amplifier gain, assumed $C = +1$ for EKF1 and $C = -1$ for EKF2, corresponding to the transmitter part

W measurement noise covariance

Detection Using SDRE

In our second approach, we set up an SDRE estimator using the following equations:

The nonlinear dynamics is rewritten to have the following structure:

$$x_{k+1} = A_k(x_k)x_k$$
$$y_k = C \cdot x_k + w_k \tag{6}$$

$f(x_k) = A_k(x_k)x_k$. Let P_k be the unique positive definite solution of the discrete-time algebraic Riccati equation:

$$P_k = A_k P_k A_k^T - A_k P_k C^T (C_k P_k C_k^T + W)^{-1} C P_k A_k^T \tag{7}$$

The SDRE filter gain is updated by:

$$K_k = A_k P_k C^T (C_k P_k C^T + W)^{-1} \tag{8}$$

Propagating from time step k to (k+1):

$$\hat{x}_{k+1} = A_k(\hat{x}_k)\hat{x}_k + K_k(y_k - C \cdot \hat{x}_k) \tag{9}$$

where $C = +1$ for SDRE Filter 1 and $C = -1$ for SDRE Filter 2. The noise covariance is W.

Detection Using UKF

In our third approach, we set up a UKF estimator using the following equations:

System model: Since x_k is the scalar state, n equals 1, κ equals 2 in our case, satisfying the condition $n + \kappa = 3$.

Propagation from time step k to (k+1):

In time update part, the 1-dimensional (n=1) x_k with mean $\hat{x}_k^+$ and covariance P_k^+ is approximated by (2n+1) weighted samples or sigma points selected by:

$$\begin{cases} x_k^{(0)} = \hat{x}_k^+ \\ x_k^{(i)} = \hat{x}_k^+ + \tilde{x}^{(i)}, i = 1,...2n \\ \tilde{x}^{(i)} = \left(\sqrt{(n+\kappa)P_k^+}\right)_i^T, i = 1,...,n \\ \tilde{x}^{(n+i)} = -\left(\sqrt{(n+\kappa)P_k^+}\right)_i^T, i = 1,...,n \end{cases} \tag{10}$$

$\left(\sqrt{(n+\kappa)P_k^+}\right)_i$ is the i^{th} row or column of the matrix square root of $(n+\kappa)P_k^+$, and the (2n+1)weighting coefficients are given as:

$$\begin{cases} W^{(0)} = \dfrac{\kappa}{n+\kappa} \\ W^{(i)} = \dfrac{1}{2(n+\kappa)}, i = 1,...,2n \end{cases} \tag{11}$$

Each sigma point is initiated through the process model:

$$x_{k+1}^{(i)} = f(x_k^{(i)}) \tag{12}$$

The predicted mean is computed by:

$$\hat{x}_{k+1}^- = \sum_{i=0}^{2n} W^{(i)} \cdot x_{k+1}^{(i)} = \frac{1}{n+\kappa}\left\{\kappa \cdot x_{k+1}^{(0)} + \frac{1}{2}\sum_{i=1}^{2n} x_{k+1}^{(i)}\right\}. \tag{13}$$

The predicted covariance, which is the a priori error covariance, is computed as:

$$\begin{aligned} P_{k+1}^- &= \sum_{i=0}^{2n} W^{(i)} \cdot (x_{k+1}^{(i)} - \hat{x}_{k+1}^-) \cdot (x_{k+1}^{(i)} - \hat{x}_{k+1}^-)^T \\ &= \frac{1}{n+\kappa}\left\{\begin{array}{l} \kappa \cdot (x_{k+1}^{(0)} - \hat{x}_{k+1}^-) \cdot (x_{k+1}^{(0)} - \hat{x}_{k+1}^-)^T + \\ \frac{1}{2}\sum_{i=1}^{2n}(x_{k+1}^{(i)} - \hat{x}_{k+1}^-) \cdot (x_{k+1}^{(i)} - \hat{x}_{k+1}^-)^T \end{array}\right\} \end{aligned} \tag{14}$$

The measurement update equations are computed as follows. Each predicted observation point is initialized using the given observation model. The state variables are the sigma points from the time update part shown above.

$$y_{k+1}^{(i)} = C \cdot x_{k+1}^{(i)} \tag{15}$$

The predicted observation is calculated by:

$$\hat{y}_{k+1} = \sum_{i=0}^{2n} W^{(i)} \cdot y_{k+1}^{(i)} = \frac{1}{n+\kappa}\left\{\kappa \cdot y_{k+1}^{(0)} + \frac{1}{2}\sum_{i=1}^{2n} y_{k+1}^{(i)}\right\} \tag{16}$$

Since the measurement noise is AWGN with covariance W, the covariance of the predicted measurement is:

$$\begin{aligned} P_y &= W + \sum_{i=0}^{2n} W^{(i)} \cdot (y_{k+1}^{(i)} - \hat{y}_{k+1}) \cdot (y_{k+1}^{(i)} - \hat{y}_{k+1})^T \\ &= W + \frac{1}{n+\kappa}\left\{\begin{array}{l} \kappa \cdot (y_{k+1}^{(0)} - \hat{y}_{k+1}) \cdot (y_{k+1}^{(0)} - \hat{y}_{k+1})^T + \\ \frac{1}{2}\sum_{i=1}^{2n}(y_{k+1}^{(i)} - \hat{y}_{k+1}) \cdot (y_{k+1}^{(i)} - \hat{y}_{k+1})^T \end{array}\right\} \end{aligned} \tag{17}$$

The cross correlation is determined by:

$$\begin{aligned} P_{xy} &= \sum_{i=0}^{2n} W^{(i)} \cdot (x_{k+1}^{(i)} - \hat{x}_{k+1}^-) \cdot (y_{k+1}^{(i)} - \hat{y}_{k+1})^T \\ &= \frac{1}{n+\kappa}\left\{\begin{array}{l} \kappa \cdot (x_{k+1}^{(0)} - \hat{x}_{k+1}^-) \cdot (y_{k+1}^{(0)} - \hat{y}_{k+1})^T + \\ \frac{1}{2}\sum_{i=1}^{2n}(x_{k+1}^{(i)} - \hat{x}_{k+1}^-) \cdot (y_{k+1}^{(i)} - \hat{y}_{k+1})^T \end{array}\right\} \end{aligned} \tag{18}$$

Finally, the measurement update of the state can be performed by regular Kalman filter equations as:

$$\begin{cases} K_{k+1} = P_{xy} \cdot P_y^{-1} \\ \hat{x}_{k+1}^{+} = \hat{x}_{k+1}^{-} + K_{k+1}(y_{k+1} - \hat{y}_{k+1}) \\ P_{k+1}^{-} = P_{k+1}^{-} - K_{k+1} P_y K_{k+1}^T \end{cases} \quad (19)$$

The amplifier gain $C = +1$ for UKF1 and $C = -1$ for UKF2.

The three nonlinear estimators presented above are used alternatively for state estimation. After the estimation, both of the resulting estimation error signals from the estimators designed above are sent to the error comparison and decision-making module. At this stage, we compare the sum of absolute values of the two estimation error signals e_1, e_2 during each symbol period. The criterion for decision making for the transmitted information symbol is given as follows:

$$output\ symbol = \begin{cases} +1, & if \sum |e_1| \le \sum |e_2| \\ -1, & if \sum |e_1| > \sum |e_2| \end{cases} \quad (20)$$

where the summations are taken over the symbol period. At this point, two important definitions, which will be used later, are given:

Definition of Minimum Distance [10]:

$d_{\min} = \min_{i \neq j} \| x_i - x_j \|, \forall i, j$, where x_i, x_j are two data symbols in a signal constellation $x = \{x_i\}_{i=0,\ldots,M-1}$. (21)

Definition of Union Bound [10]:

The probability of error for the ML (Maximum Likelihood) detector on the AWGN channel, with M–point signal constellation with minimum distance $d_{\min}(x)$, is bounded by $P_e \le (M-1) \cdot Q\left[\frac{d_{\min}}{2\sigma}\right]$, where the Q function is defined by:

$$Q(z) = P(x \ge z) = \int_z^{\infty} \frac{1}{2\pi} \cdot e^{-x^2/2} dx \text{ and } \sigma^2 = N_0 / 2 . \quad (22)$$

Therefore, the larger the minimum distance is, the less probability of error occurs.

III. NUMERICAL RESULTS

In order to apply the minimum distance and union bound introduced in the last section, to explain the experimental results, we must guarantee that the estimated state variables approximately obey the Gaussian distribution. The following computer experiment involving the symmetric tent map parameter estimation is used to demonstrate this Gaussian distribution property. The symmetric tent map and its measurement equation can be written as:

$$\begin{cases} x_{k+1} = a - 1 - a \cdot |x_k| \\ y_k = C \cdot x_k + w_k \end{cases} \quad (23)$$

The parameter a is between 1 and 2 for chaotic behavior. By incorporating the parameter a into the state vector, we apply EKF to estimate its probability density function. We choose $a = 1.8$ with different SNRs to compare the histograms (sample probability density functions) of parameter estimates, and find that the histogram is sufficiently close to a Gaussian distribution. Then, we find that this quasi-Gaussian distribution is independent of the selection of parameter a.

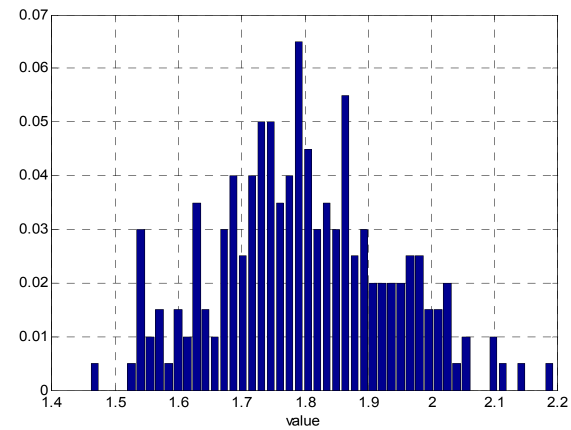

Fig.3. Histogram of the estimated parameter distribution with SNR=30 and a=1.8

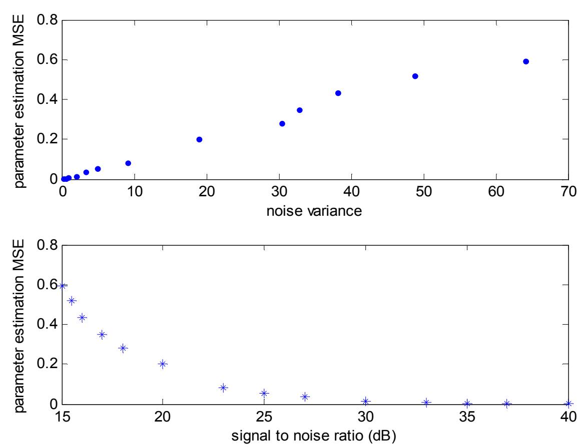

Fig.4. Relationship between parameter estimation MSE with noise variance

Fig.3 shows the histogram of the estimated symmetric tent map parameter with SNR=30dB and a=1.8. And Fig.4 shows the existing linear relationship between the parameter estimation mean square error and noise variance. Therefore, this experiment demonstrates the approximate Gaussian distribution property of the estimated parameter, and shows that union bound theory can be applied to explain our simulation results.

Example 1: Symmetric tent map is used to demonstrate the performance comparison of the three communication schemes: two previous ones [4]-[6] and our proposed scheme. In the first scheme: parameter estimation based demodulation, the two parameters are $a1 = 1.95$ and $a2 = 1.55$. The parameter range in the symmetric tent map is very small, therefore the minimum distance is relatively small compared with the other two schemes, in our example, $d_{\min} = a1 - a2 = 1.95 - 1.55 = 0.4$, which limits the performance of the first scheme. The second scheme using two maps technique shows improvement over the first scheme, since it has larger minimum distance. Our new chaotic communication scheme always guarantees the largest minimum distance $d_{\min} = 2 \cdot \sqrt{E_b}$ among the three schemes, therefore, it gives superior BER performance, as shown in Figs.5 and 6.

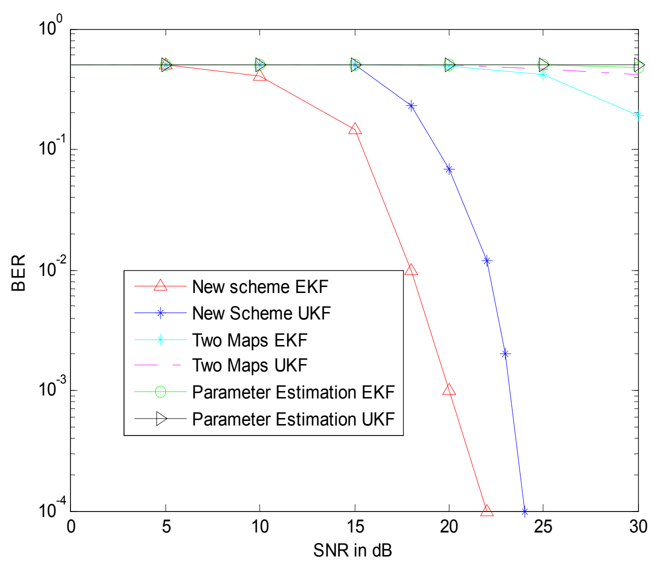

Fig.5.Communication with symmetric tent map BER performance 1

Fig.6 shows the performance of the SDRE estimator for the symmetric tent map. This performance is close to that of EKF. In this simulation, we need the factorization process $f(x_k) = A_k(x_k)x_k$, but $A_k(x_k)$ can be a very large value when x_k is close to zero. Therefore, in order to make sure SDRE is still working, we need to set up an upper bound on $A_k(x_k)$ in this condition, which also limits the tracking performance of the SDRE in this application. Both Fig.5 and Fig.6 show that our new chaotic communications using EKF provides us the best BER performance among all these results. As mentioned before, the superior performance is due to its inherent largest minimum distance.

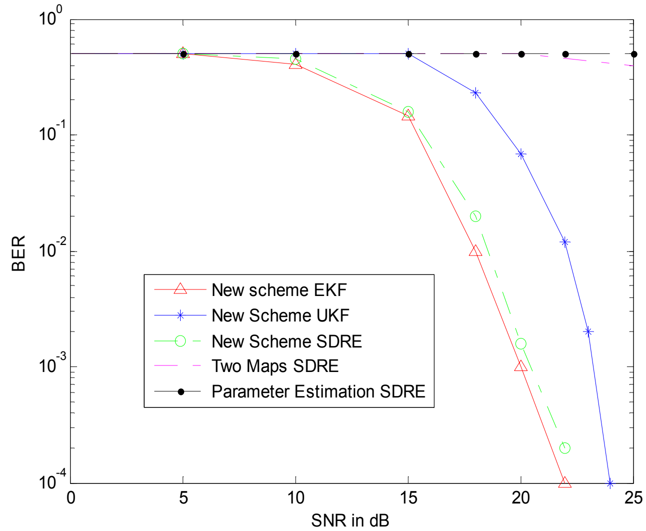

Fig.6. Communication with symmetric tent map BER performance 2

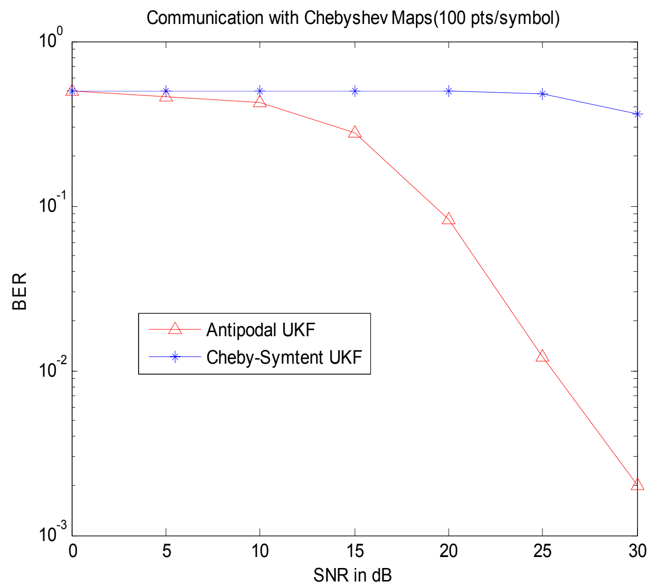

Fig.7. Communication with the 2nd order Chebyshev map BER performance

Example 2: We simulate the BER performance of the chaotic communication using the 2nd order Chebyshev map, as shown in Fig.7. The 2nd order Chebyshev map and its measurement equation can be written as:

$$\begin{cases} x_{k+1} = 2x_k^2 - 1 \\ y_k = C \cdot x_k + w_k \end{cases} \tag{24}$$

Simulation results show that the EKF based schemes do not produce reliable convergence, but the UKF based schemes produce satisfactory results. Our new scheme using UKF still shows better performance compared with the two map based estimation scheme using UKF with the 2nd order Chebyshev map and the symmetric tent map. We did not include the parameter estimation based communication scheme since there is no parameter which can be changed in the Chebyshev map. We have also tried the SDRE estimator. However, it cannot provide a non-negative solution for the discrete algebraic Riccati equation at every time step.

It is expected that the filter with the matched model tracks the chaotic sequence, and the filter with the unmatched model produces more estimation error. However, simulation results show that, even with the erroneous system model, UKF still tracks the signal quite well by using nonlinear transformation of the sigma points, which is not quite desirable in this special case. However, we must notice that although our new scheme using the EKF gives the best performance for symmetric tent map, it is still subject to the stability issues of EKF in estimation of the state of the nonlinear chaotic map [11], since it employs EKF for detection. For severely nonlinear chaotic maps, the EKF and SDRE based methods may give unreliable filtering performance, and the UKF based methods can provide good tracking performance.

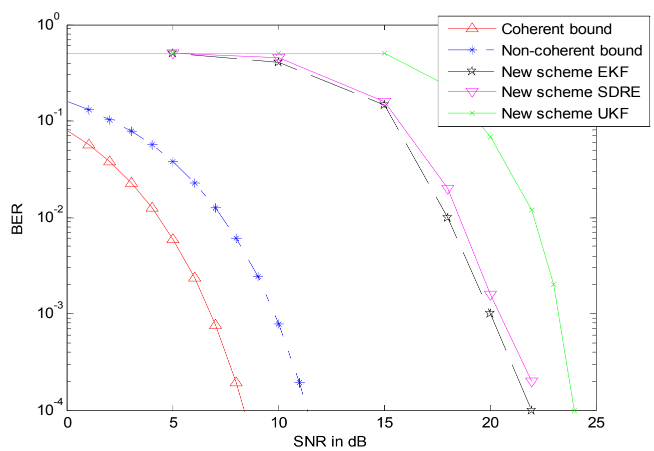

Fig.8. Theoretical bound of chaotic communications

IV. General Performance Analysis

Let us discuss the theoretical performance bound for chaotic communications. For coherent reception, such as our new chaotic communication scheme, the minimum distance $d_{\min} = 2 \cdot \sqrt{E_b}$. For binary transmission $M = 2$, the union bound is given as follows, by using Eqn. (22).

$$P_{coherent} \le Q\left[\frac{d_{\min}}{2\sigma}\right] = Q\left[\sqrt{\frac{2E_b}{N_0}}\right] = \frac{1}{2} erfc\left(\sqrt{E_b / N_0}\right)$$

where $erfc(z) = 1 - erf(x) = \dfrac{2}{\sqrt{\pi}} \displaystyle\int_z^{\infty} e^{-t^2} dt$. (25)

For non-coherent reception, such as the COOK, the minimum distance $d_{\min} = \sqrt{E_b}$. Therefore, the performance of non-coherent reception is given by

$$P_{non-coherent} = \frac{1}{2} erfc\left(\sqrt{E_b / 2N_0}\right). \qquad (26)$$

Fig.8 shows the comparison of our results with what is theoretically possible to achieve. Although our new scheme greatly improves the BER performance compared with other chaotic communication schemes, there still exists room for improvement to meet the theoretical performance bound.

V. Conclusions

We have presented a novel nonlinear-filtering-based modulation/demodulation technique for chaotic communications. We have compared its bit error rate performance with other existing nonlinear filtering based schemes. The EKF, SDRE and UKF filters are set up separately for state estimation performance comparison. It is found that our new scheme using EKF provides the best BER performance in these examples. The theoretical BER performance bounds for chaotic communications are also given in this paper for comparison purposes. With reasonable computational complexity and superior BER performance, our new digital chaotic communication scheme shows superior applicability in the UWB communications.

References

[1] W. M. Tan, F. C. M. Lau, C.K. Tse, *Digital Communications with Chaos --- Multiple Access Techniques and Performance,* Elsevier, 2007.

[2] IEEE 802.15.4a Task Group, *WPAN Low Rate Alternative PHY*, online available at http://www.ieee802.org/15/pub/TG4a.html.

[3] Y. H. Kim, et. al., *Chaotic UWB System*, IEEE 802.15-05-0132-03-004a, Monterey, CA, USA, March, 2005. http://grouper.ieee.org/groups/802/15/pub/05/15-05-0132-03-004amerged-proposal-chaotic-uwb-system-802-15-4a.pdf

[4] H. Ruan, T. Zhai and E. E. Yaz, "A Chaotic Secure Communication Scheme with Extended Kalman Filter Based Parameter Estimation," *Proc. of 2003 IEEE Conf. on Control Applications*, Istanbul, Turkey, pp. 404-408, 2003.

[5] H. Ruan, T. Zhai, and E. Yaz, "A Demodulation Scheme Based on State Estimation for Chaotic Digital Communications," *Proc. of the American Control Conf.*, Denver, Colorado, pp.1614-1619, 2003.

[6] H. Ruan, E. E. Yaz, T. Zhai, and Y. I. Yaz, "A Generalization of Tent Map and its Use in EKF Based Chaotic Parameter Modulation/Demodulation," *43rd IEEE Conf. on Decision and Control*, Atlantis, Paradise Island, Bahamas, pp. 2071-2075, 2004.

[7] F. O. Hounkpevi and E. E. Yaz, "An Improved Nonlinear-Estimation Based Chaotic Communication Scheme," *IEEE International Conf. on Control Applications*, Munich, Germany, pp. 1426-1431, 2006.

[8] J. R. Cloutier, "State-Dependent Riccati Equation Techniques: An Overview," *Proceedings of the American Control Conference*, Albuquerque, NM, pp.932-936, 1997.

[9] S. J. Julier, J. K. Uhlmann, "Unscented Filter and Nonlinear Estimation", *Proceedings of the IEEE*, Vol. 93, No. 3, pp. 401-422, 2004.

[10] J. M. Cioffi, *Digital Communication–Signal Processing*, unpublished lecture notes, available at: http://www.stanford.edu/class/ee379a, Stanford University.

[11] K. Reif, S. Gunther, E. Yaz, and R. Unbehauen, "Stochastic Stability of the EKF: the Discrete-Time Case," *IEEE Trans. on Automatic Control*, vol.44, pp. 714-728, 1999.